



The Effect of Strain Rate and the Chemical Effects of H₂ and CO on the Soot Formation of Ethylene-Syngas in Opposed Jet Laminar Diffusion Flame

Brakchi Mohamed Seghaier¹, Hadeef Amar^{1,2*}, Mameri Abdelbaki^{1,2}, Aouachria Zeroual³

¹ Mechanical Engineering Department, SASF, University Larbi Ben M'Hidi of Oum El Bouaghi, Oum El Bouaghi 04000, Algeria

² CMASMTF Laboratory, University Larbi Ben M'Hidi of Oum El Bouaghi, Oum El Bouaghi 04000, Algeria

³ Applied Energy Physics Laboratory (AEPL), Faculty of Material Sciences, University Batna1, Batna 05000, Algeria

Corresponding Author Email: hadeef.amar@univ-oeb.dz

<https://doi.org/10.18280/ijht.410205>

ABSTRACT

Received: 7 November 2022

Accepted: 12 February 2023

Keywords:

opposed flow, strain rate, soot, method of moments, flame temperature, chemical effect

In this work, the effects of the composition of the syngas, the deformation rate and the chemical effect of H₂ and CO on the internal structure of the flame as well as the soot formation, in a laminar diffusion flame of a syngas mixture / ethylene. The configuration has two opposite jets and is used at an interval of the ignition deformation rate at extinction under atmospheric pressure. Chemistry in the gas phase is coupled according to the soot model based on polycyclic aromatic hydrocarbons (PAH), by the moment's method. The insertion of the inactive species FH₂ and FCO will also be included to determine the chemical effect of H₂ and CO. The results have shown that the increase in hydrogen in the syngas leads to a decrease in the growth rates of the soot in dilution effect as well as by chemical effects due to the abolition of the abstraction reaction of H in the hydrogen-addition hydrogen abstraction sequence of C₂H₂.

1. INTRODUCTION

Soot is a by-product of an incomplete hydrocarbon combustion process that has been of global concern in recent years because of its effect on global warming and human health. Therefore, its reduction has become essential.

On this perspective, numerous studies have been launched on the soot training mechanism and the tools to reduce it [1]. Many chemical and physical phenomena in the formation of soot, are not yet fully understood. The pyrolysis of hydrocarbons fuels leads to the formation of soot precursors in the flame area, such as acetylene and propargyl which gives the benzenic cycle. Before the soot formation, the Hydrogen-Additional Addition mechanism of C₂H₂ (HACA), established by Appel et al. [2], plays an important role in the growth of polycyclic aromatic hydrocarbons (PAH).

In areas where the presence of oxygen is important in an opposed jet configuration, the axial distribution of the soot is non-monotonous relative to the oxygen concentration. Then the reduction in the volume fraction of the soot is linked to the elimination of the birth of soot and favored phenomenon of oxidation of the soot through the critical value the of oxygen fraction [3]. Several works have shown that the dilution of the fuel or oxidizer by non-combustible elements (N₂, H₂O and AR), or fuel such as (H₂ and CO) affects the soot formation by four important mechanisms which are the attenuation effect that modifies the total mass oxidation of the fuel, the thermal effect resulting from modifications of the thermal properties of the reagents and the chemical effect of the reactive diluent during participation in chemical reactions [4, 5].

Hydrogen represents the cleanest energy vector. To improve the efficiency of the flame and the reduction of pollutants, it is widely used as a doping substance [6]. In previous studies,

Wang et al. [7] have studied the chemical impact of hydrogen on soot formation and analyse the main training paths of benzene and Pyrene (C₁₆H₁₀) to see how hydrogen affects its composition in the flames of methane and ethylene.

They have concluded that added hydrogen improves the storage of the soot in the methane flame by producing H and C₂H₂, which leads to the formation of the first aromatic cycle by the HACA mechanism. On the other hand, the addition of hydrogen to the C₂H₄ flame reduces the nucleation rate and the growth rate on the surface of the soot. An experimental and numerical investigation was carried out by Zhang et al. [8], in laminar diffusion flames of ethylene/air, with a variation in the content of O₂ in the oxidant from 21% to 50% and a replacement of N₂ by CO₂. They studied the internal structure of the flame and the soot formation by the chemistry model C₂. The increase in the quantity of oxidant causes high flame temperatures and a rapid increase in the volume fraction of soot with a displacement of the upper center of flame. The thermal and chemical effects of CO₂ reduce the formation of soot, the formation of species C₂H₂, C₆H₆ and C₁₆H₁₀ are affected by the replacement of N₂ by the CO₂ in oxidant. The effect of hydrogen and nitrogen on the soot formation in an ethylene-air flame using the COFLAM code was carried out by Khanehzar et al. [9]. Also, the authors studied various effects of chemical, thermal and transport hydrogen on the structure of the flame and the formation of soot. The results have shown that adding hydrogen and nitrogen reduced the radiation and the volume of soot; they concluded that the HACA mechanism and the PAH condensation rate were responsible of this decrease. The work of Liu et al. [10], shown that hydrogen enrichment increases the production of free radicals H and OH by the chain ramification reaction H₂ + O=H + OH. Since the radical H has increased the growth on

the surface of the soot according to the HACA mechanism which leads to the increase in the concentrations of acetylene and propargyl. Latter generates the benzene by a recombination reaction.

Ying et al. [11] conducted a detailed study of the chemical effect of hydrogen on soot formation in a methane flame with air. He It was concluded that adding hydrogen reduces the production of acetylene (C_2H_2), Ketene (CH_2CO) and increases the concentrations of H, OH and O. Moreover, radical H directly affects the growth of the soot surface through the HACA mechanism. Wei et al. [12] studied the effect of adding hydrogen (0%, 20% and 40%) on soot formation using the Monte-Carlo method to solve the dynamic particle model, the coagulation and surface reaction. The results have shown that the molar concentrations of significant soot species, such as C_2H_2 and PAH, are inhibited by the increase in hydrogen in the fuel. Consequently, the volume fraction of the soot was reduced. In the last decade, research has concluded that syngas can be used as a source of hydrogen. Syngas is an organic fuel composed mainly of hydrogen and carbon monoxide, its addition to a hydrocarbon improves the quality of combustion and reduces emissions [13]. An experimental study of an opposed jet methane/ ethylene flame was carried out by Xu et al. [14] to elucidate the impact of hydrogen on the soot formation. The results obtained show that the role of the chemical effect of hydrogen in the formation of soot depends not only on the type of fuel (ethylene or methane), but can also be sensitive to the composition of the oxidizer.

The objective of this paper is to study the effects of the composition of the syngas, the strain rate on the internal structure of the flame as well as the soot formation, in a laminar diffusion flame opposed to a syngas mixture / ethylene. The inactive species FH_2 and FCO will also be included to determine their chemical effect. The reason for the choice of C_2H_4 as a fuel is based on the fact that ethylene plays an important role in the oxidation of large hydrocarbons.

2. CONFIGURATION AND CALCULATION METHOD

The axisymmetric geometry with two opposed jets with an asymmetric geometry is used (Figure 1), mathematically that means that all derivatives in the third direction theta vanish $\frac{\partial}{\partial \theta} = 0$. This configuration allows the formation of a diffusion flat stationary flame between the two injectors. The structure of the flame is supposed to be uniform in the longitudinal direction of the flame (direction r), this assumption gives a one-dimensional flame with properties depending only on the cross direction (direction x). It consists of two opposite nozzles with a distance $D=2.9$ cm, one injecting an Ethylene / Syngas mixture and the other oxidizing it with a temperature of 300 K (Table 1 and 2).

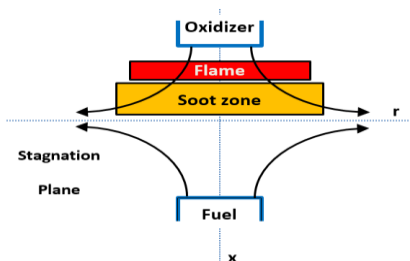


Figure 1. Geometric configuration of an opposed jet

Table 1. Fuel composition: Volumetric composition mixtures

The denomination	C_2H_4	H_2	CO
F01	0.40	0.15	0.45
F02	0.40	0.20	0.40
F03	0.40	0.25	0.35
F04	0.40	0.30	0.30

Table 2. Oxidizer composition

O_2	N_2
0.21	0.79

In order to ensure that the stagnation plane was in the center, the momentum ratio of the species to the opposing nozzles was the same. Eq. (1) shows the definition of the global strain rate [15].

$$a = \frac{2(-u_O)}{L} \left[1 + \frac{u_F}{(-u_O)} \sqrt{\frac{\rho_F}{\rho_O}} \right] \quad (1)$$

where, the index O represents the oxidant, F the fuel, u is the speed in the x direction, of ρ is the density, as well as the overall strain rate a .

The description of the equations governing the opposite flow flame model is as follows [16]. The mass conservation equation is:

$$\frac{\partial(\rho u)}{\partial x} + \frac{1}{r} \frac{\partial(\rho v r)}{\partial r} = 0 \quad (2)$$

where, u and v are the axial and radial velocity components, respectively.

With $G(x) = \frac{-\rho r}{r}$ and $F(x) = \frac{\rho u}{2}$ the continuity Eq. (1) becomes:

$$G(x) = \frac{dF(x)}{dx} \quad (3)$$

The equation of conservation of momentum is written:

$$H - 2 \frac{d}{dx} \left(\frac{FG}{\rho} \right) + \frac{3G^2}{\rho} + \frac{d}{dx} \left[\mu \frac{d}{dx} \left(\frac{G}{\rho} \right) \right] = 0 \quad (4)$$

With

$$H = \frac{1}{r} \frac{dP}{dr} \quad (5)$$

The energy conservation equation is:

$$\rho u \frac{dT}{dx} - \frac{1}{c_p} \frac{d}{dx} \left(\lambda \frac{dT}{dx} \right) + \frac{\rho}{c_p} \sum_k c_{pk} Y_k V_k \frac{dT}{dx} + \frac{1}{c_p} \sum_{k=1}^K h_k \dot{\omega}_k - \frac{\dot{q}_r}{c_p} = 0 \quad (6)$$

The species conservation equation is:

$$\rho u \frac{dY_k}{dx} + \frac{d}{dx} (\rho Y_k V_k) - \dot{\omega}_k W_k = 0 \quad (7)$$

where, v is the speed in the direction r , cp is the specific heat capacity at constant pressure, λ is the coefficient of thermal conductivity, Y_k is the mass fraction of the k species, V_k is the rate of diffusion of the k species, h_n is the specific Enthalpy of the k^{th} species, and W is the molecular mass of the k^{th} species.

The effects of radiation per unit volume are taken into account by:

$$\dot{q}_r = -4\sigma K_P(T^4 - T_\infty^4) \quad (8)$$

p is the species affected by the radiation, namely CO_2 , H_2O , CO and CH_4

$$K_P = P_{\text{CO}_2}K_{\text{CO}_2} + P_{\text{H}_2\text{O}}K_{\text{H}_2\text{O}} + P_{\text{CO}}K_{\text{CO}} + P_{\text{CH}_4}K_{\text{CH}_4} + \kappa_{\text{particle}} \quad (9)$$

where, σ is Stefan Boltzmann's constant, T and T_∞ are the local and ambient temperatures, respectively, K_P is the average absorption coefficient. P_k and K_k are the partial pressure and the mean absorption coefficient of species k , κ_{particle} is the soot absorption coefficient [17], which is proportional to the volume fraction of soot:

$$\kappa_{\text{particle}} = 1307 \cdot f_v \cdot T \quad (10)$$

The soot formation is modeled by a statistical method (Method of moments) established by Frenklach [18]. The entire quantity x_i^r which is weighted by a probability density function p_i :

$$M_r = \sum_{i=1}^{\infty} x_i^r \cdot N_i \quad (11)$$

The probability density function is taken equal to the concentration of class particles i N_i . The size x_i^r is linked to the mass where the mass $m_i = i \cdot m_1$ and m_1 of the small particle of soot represents, so the moment M_r of order r becomes:

$$M_r = \sum_{i=1}^{\infty} i^r \cdot N_i \quad (12)$$

With the first moment M_0 corresponds to the total concentration of the particles while the volume fraction of soot f_v is calculated by the second moment:

$$M_1 = \sum_{i=1}^{\infty} i \cdot N_i = \sum_{i=1}^{\infty} \frac{m_i}{m_1} \cdot N = f_v \cdot \frac{\rho_s}{m_1} \quad (13)$$

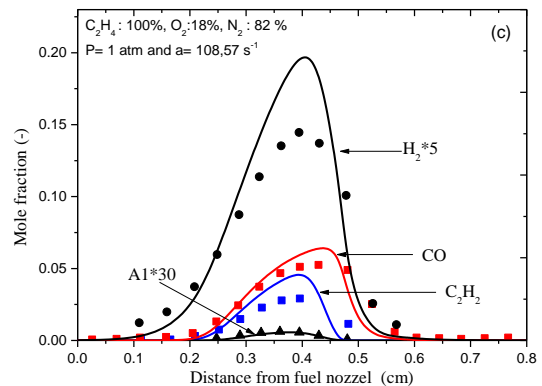
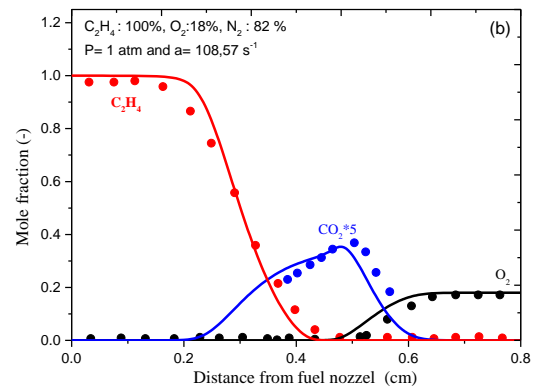
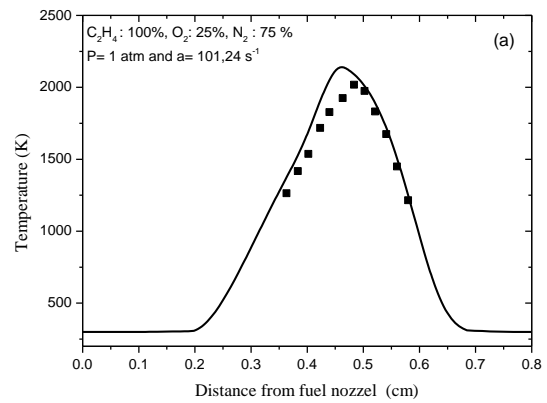
ρ_s represents the density of the soot particle.

Chemkin's Oppdiff program established by Kee et al. [19] is used for solving flow equations for chemical kinetics, the reaction mechanism developed by Appel et al. [20] which is composed of 101 species and 543 reactions which include PAH growth reactions until pyrene is adopted.

3. VALIDATION

The configuration with opposite jets has been used in several studies with different fuels and oxidants. The investigation of Zhou et al. [21] is carried out on an experimental installation which consists of two opposite nozzles of interior diameter of 10 mm separated by a distance of 8 mm. The ethylene is ejected from on the lower side with a speed of 21.6 cm/s, while the oxidant is ejected from by the upper side with a speed of 22.1 cm/s. The oxidizer and fuel have the same temperature and initial pressure, which are respectively 300K and 1 atm.

Figure 2 represents flame temperature profiles and molar fractions along the axial distance, the consumption of species such as C_2H_2 and O_2 , the production of minor and major species (CO_2 , CO , H_2 , C_2H_2) and the soot volume fraction. All these species are well predicted, according to experimental measures.



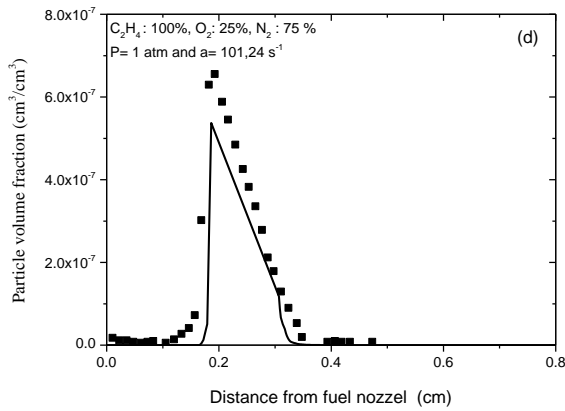


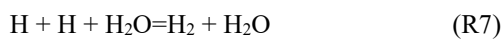
Figure 2. Temperature and species profiles (Experimental results (symbols) and prediction(lines))

4. RESULTS AND DISCUSSION

4.1 The effects of hydrogen and the strain rate on the maximum flame temperature

Depending on the different compositions of the mixture (Table 1), the variation in the maximum combustion temperature at a constant pressure $P=1$ atm as a function of the strain deformation rate is illustrated in Figure 3 (a). Monotonous temperature growth is observed to reach maximum value at a strain rate equal to 18 s^{-1} , then it decreases to an extinction point. The latter differs from one mixture to another, depending on the quantity of H_2 in the mixture, which increases the resistance of the flame to stretch [22]. The amount of hydrogen, which varies in volume from 15% to 30% in the mixture, increases influences significantly on the rise in temperature peak.

Elementary reactions cited in interpretations are:



The maximum flame temperature (T_{max}) increases when the hydrogen fraction increases in the syngaz. Decomposition of hydrogen provides a pool of free radicals such as H and OH

according the elementary reactions: R2, R3, R5, R6 and R7 that increase species diffusion and reactivity as shown in the Figure 3 (b). The increase percentage of temperature with hydrogen added to the fuel (from mixture F1 to F4) ranges from 1.04 % at a strain rate of 200 s^{-1} to 2.13 % at a strain rate of 18 s^{-1} .

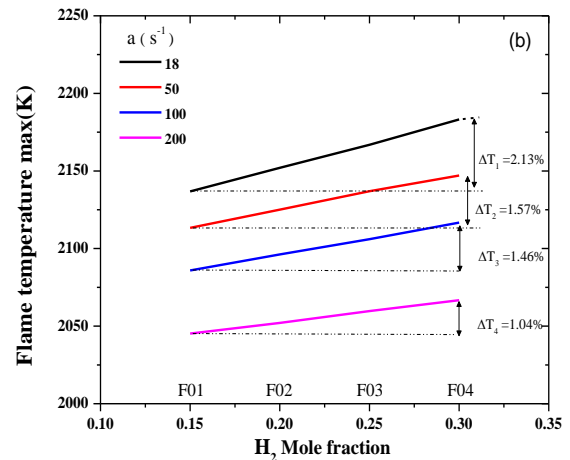
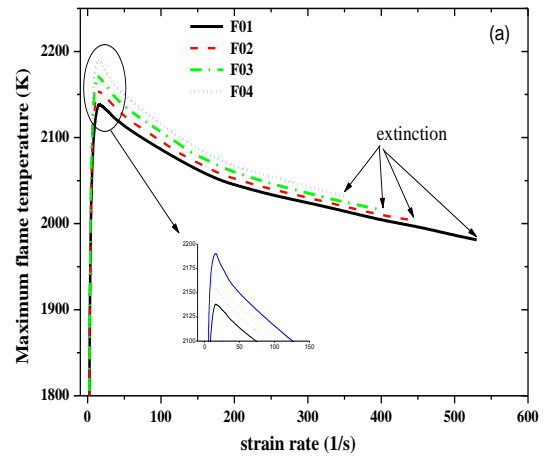


Figure 3. Variation of the maximum flame temperature with the deformation rate and the quantity of hydrogen

4.2 Internal structure of flame and soot formation

To analyse the effect of the strain rate on the soot formation and internal flame structure, the extreme cases of the mixtures, namely F1 and F4, are represented in terms of axial temperature and major species profiles. Two values of strain rate are considered, a relatively low and high ones (18 s^{-1} and 100 s^{-1}). At a train rate of 18 s^{-1} , when hydrogen volume is 15% in the mixture F1, the position of the maximum value of the flame temperature, which represents the flame front noted by $X_{T_{\text{max}}}$, is located at a distance $X_{T_{\text{max}}}=1.57$ cm from the fuel nozzle, Figure 4 (a). Whereas, while strain rate increases to 100 s^{-1} (Figure 4 (b)), the flame front shifts towards the stagnation plane, where the velocity is zero, noted by $X_{p,\text{stag}}$, in this case $X_{T_{\text{max}}}=1.45$ cm. When the quantity H_2 increases in the fuel (flame F4), in the case of strain rate $a=18 \text{ s}^{-1}$, the flame front moves to $X_{T_{\text{max}}}=1.45$ cm Figure 5 (a), while the displacement Towards the stagnation plane $X_{p,\text{stag}}$ takes the value of $X_{T_{\text{max}}}=1.40$ cm Figure 5 (b) according to a deformation rate $A=100 \text{ s}^{-1}$.

The phenomenon of pyrolysis is initiated alongside the fuel, which is not far from the flame front, to produce these gaseous species such as C_2H_2 and C_3H_3 , the latter promotes the formation of benzene and the PAH which represent the pioneers of soot. The decomposition of C_2H_4 is affected by the increase in the strain rate for the two flames F01 and F04, it delays its dissociation for the value of $a=18\text{ s}^{-1}$. The dissociation phenomenon begins from the axial position $x=0.8\text{ cm}$ where the consumption of the species C_2H_4 is not fast enough Figure 4 (a). Compared to the same flame (F01), when the strain rate increases to $a=100\text{ s}^{-1}$, the dissociation position shifts to $x=1.1\text{ cm}$ and the consumption of the species is very fast Figure 4 (b).

Similarly, for the flame (F04), the dynamic effect of the strain rate affects the formation of C_2H_2 species which begin to occur from an axial position of $X=0.8\text{ cm}$ for a low deformation rate ($a=18\text{ s}^{-1}$) Figure 5 (a) to reach a maximum value, then it disappears definitively in position $X=1.5\text{ cm}$. Whereas, the production of acetylene is delayed by the increase in the strain rate for a value of $a=100\text{ s}^{-1}$ Figure 5 (B), its formation is rapid relatively to the rate $a=18\text{ s}^{-1}$, it begins at the position $x=1.05\text{ cm}$ and vanishes rapidly and definitively at position $x=1.4\text{ cm}$.

The radical C_3H_3 (propargyl) is very induced by the variation in the strain rate in the two mixtures F01 and F04. On one hand, the decrease of C_3H_3 in Figure 4 (a and b), it is mainly due to the consumption of CH_3 by the reaction R40, since CH_2 is responsible for the production of C_3H_3 by R193 [22-24]. On the other hand, the rise in the strain rate reduces the thickness of the zone of formation of these species, as well as their rapid consumption. However, the increase in the quantity of hydrogen does not represent as an essential source for the formation of the radical Propargyl C_3H_3 suspected of being at the origin of the formation of the first aromatic nuclei and the soot Figure 5 (a and b).

The stagnation plane is a surface where the axial velocity of the two jets is zero, it is noted by $X_{p.stag}$, its position is near the fuel nozzle. In this region the onset of soot nucleation occurs by soot particles such as the Benzene (A1), naphthalene (A2), Phenanthrene (A3) and pyrene (A4).

These particles are transported through the thermal flow produced by the flame to the stagnation plane. During this period, the physico-chemical process plays an important role in the growth of emerging particles to achieve maximum value near the stagnation plan, the low diffusion of particles in this stage leads to their elimination.

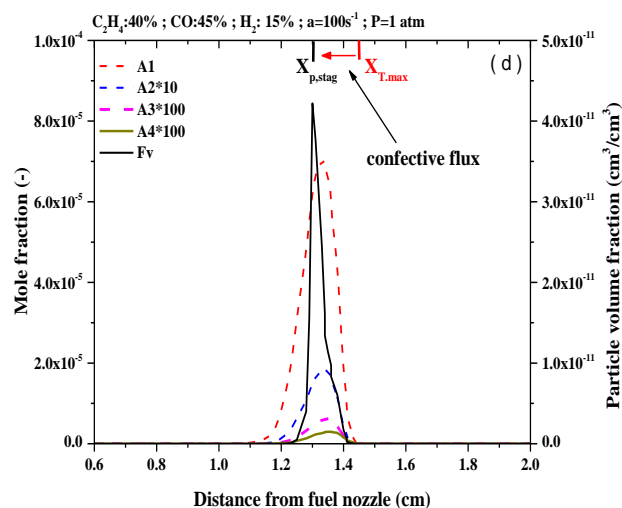
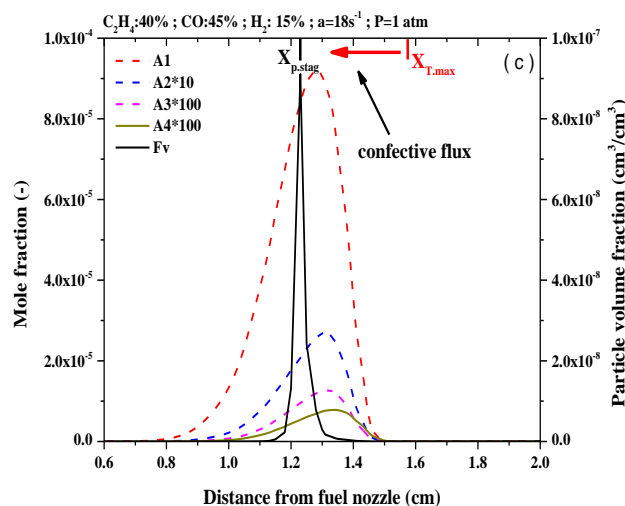
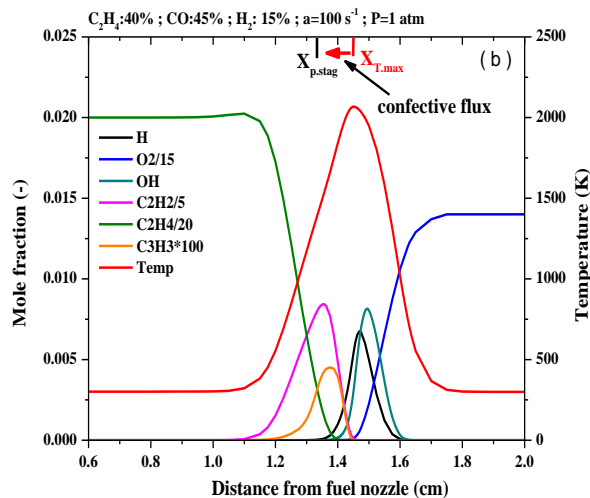
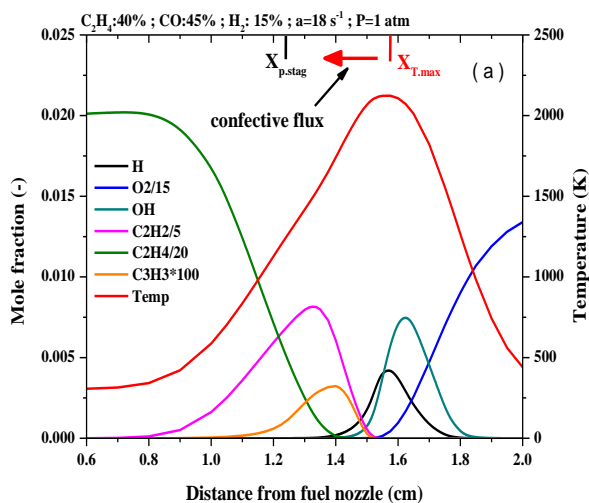


Figure 4. Axial profile of major chemicals and precursor soot and the volume fraction of soot for flame F01

According to this scenario, the molar fractions of several aromatics, such as benzene (A1), naphthalene (A2), phenanthrene (A3) and pyrene (A4) as a function of the strain rate and the volume of hydrogen in the fuel are represented. The reduction in residence time, which is represented by the increase in the strain rate, and the content of H_2 in the fuel,

reduces the formation of benzene (A1) to the value of 0.925 ppm for flame F01 for $a=18 \text{ s}^{-1}$ and to 0.705 ppm for $a=100 \text{ s}^{-1}$ Figure 4 (c and d). In the case of the F04 flame, where the quantity of hydrogen is increased, the value of A1 increases from 0.850 ppm (at $a=18 \text{ s}^{-1}$) to 0.550 ppm (at $a=100 \text{ s}^{-1}$) Figure 5 (c and d). This is mainly due to the fact that benzene is produced later by route R234. The evolution of the production and consumption of A2, A3 and A4 takes the same path as benzene.

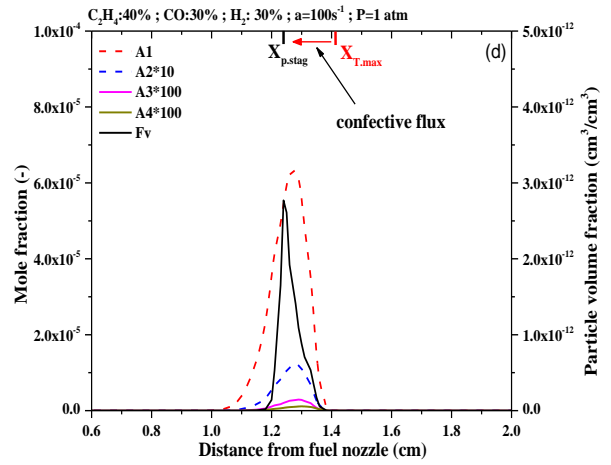
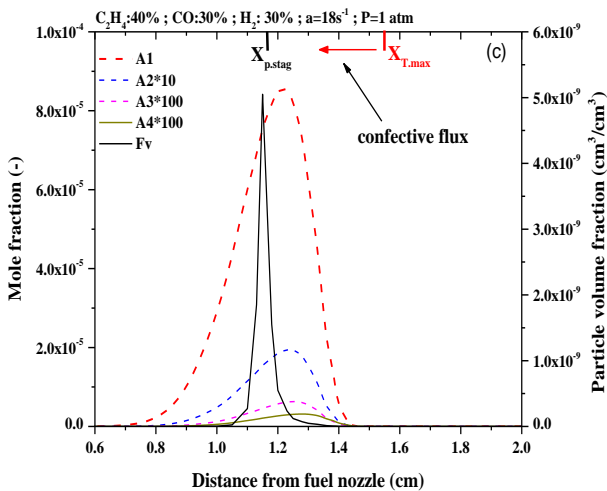
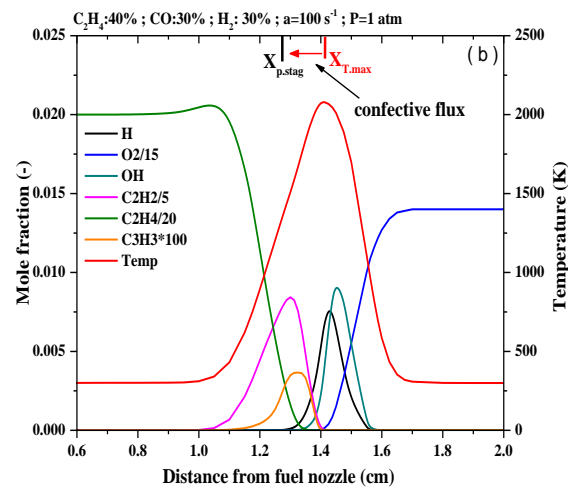
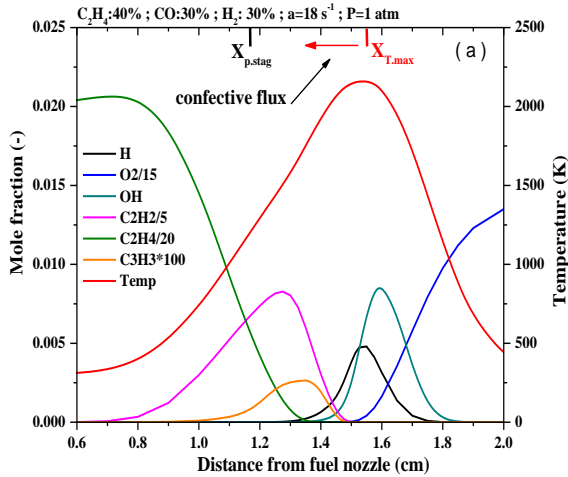


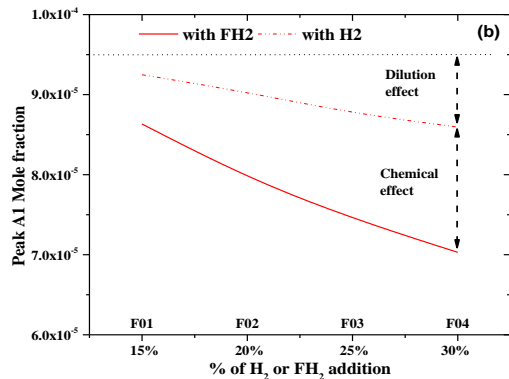
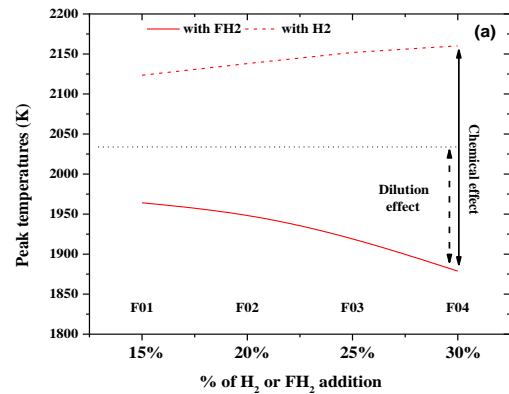
Figure 5. Axial profile of major chemicals and precursor soot and the volume fraction of soot for flame F04

According to the results obtained, we note that when the strain rate increases, the thicknesses of the flames and the maximum values of A1, A2, A3 and A4 consequently decrease, the particle volume fraction reduced in a significant manner Figure 4(c and d) and Figure 5(c and d).

4.3 H₂ and CO chemical effect on soot formation

4.3.1 H₂ chemical effect

Soot formation is directly related to soot generation and surface reactions, which are coupled with the gas phase chemistry of the flame to initiate the generation of gas phase soot precursors [23]. A discussion of the chemical effect of H₂ addition on soot formation in the F01 and F04 flames is shown in Figure 6 (a-d).



via an HACA (H-Abstraction C₂H₂-Addition) mechanism.

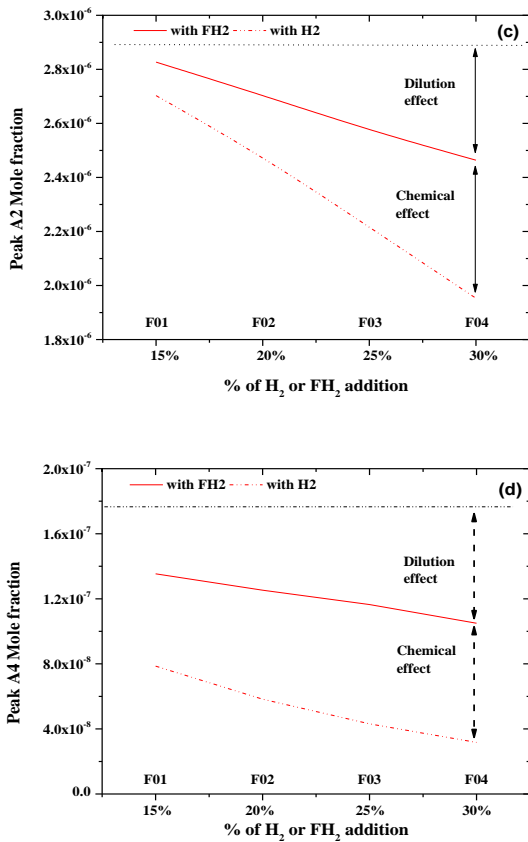


Figure 6. Chemical effects of H₂ added to the fuel side on flame temperature and soot formation

Figure 6 (a) shows that the elimination of the chemical effect of H₂ by the insertion of an inert species FH₂ plays a major role on the maximum temperature value, through the absence of H₂ reactivity which directly reduces the value of the combustion temperature. In the presence of FH₂, T_{max}=1964K and T_{max}=1878 K, while in H₂ T_{max}=2123 K and T_{max}=2160 K.

Acetylene plays a major role in the production of C₃H₃ by the reaction R193, the latter contributes in part to the formation of benzene (A1) by the dominant reaction (R234), in a direct way the elimination of the chemical effect of hydrogen which represents a link in the formation of C₂H₂ reduces the formation of benzene Figure 6(b) For naphthalene (A2) Figure 6.c it can be directly seen that it is very much induced by the chemical effect of H₂ with a gap that increases as a function of the amount added to the fuel, and for the formation of A4 this gap is constant Figure 6(d) relative to the increase of H₂ in the fuel.

4.3.2 CO chemical effect

Carbon monoxide is a reactive combustible substance with a calorific value lower than 10.90 MJ/Kg, so the elimination of the chemical effect of this substance reduces the combustion temperature and the species such as A1, A2, A4 by a significant value.

In Figure 7 (a), the maximum combustion temperature for the four flames is very much induced by the elimination of the chemical effect of CO, while this decrease is reduced proportionally to the amount of CO by volume of the mixture.

Carbon monoxide enhances the production of the soot precursor C₂H₂ via the reaction pathways R146 and R150 and the H-radical via R31, i.e., it indirectly affects soot formation

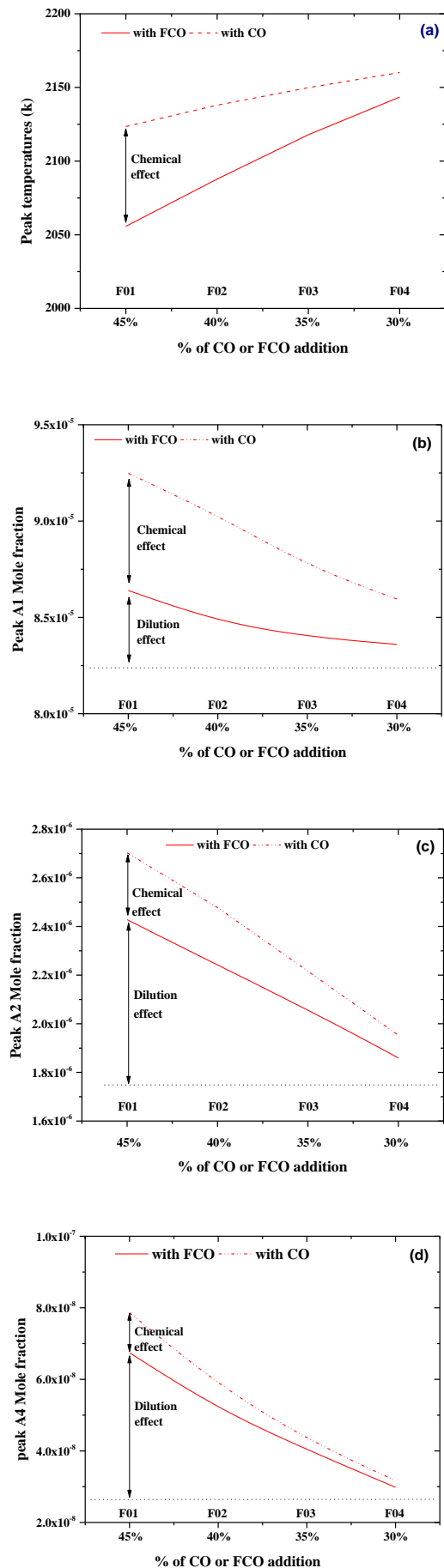


Figure 7. Chemical effects of CO added to the fuel side on flame temperature and soot formation

The latter reactions are eliminated in the absence of the chemical effect, which is why we find that when carbon monoxide is present, the soot formation process is more important than in the presence of the FCO.

Figure 7 (b) illustrates the reduction of benzene following the increase of CO in the syngas by eliminating the reactivity of carbon monoxide. This reduction is minimal for the A2 formation Figure 7 (c) and more negligible for A4 Figure 7 (d).

5. CONCLUSIONS

The effects of strain rate and mixture composition, as well as the chemical effects of hydrogen and carbon monoxide on the internal flame structure and sooting of an ethylene/syngas mixture in a jet configuration opposite, the conclusions when they can be drawn are the following:

- Displacement of the flame front which is represented by the maximum temperature towards the fuel nozzle following the increase in hydrogen in the fuel.
- The increase in the rate of deformation delays the dissociation of C₂H₄, which will impact on the formation of C₂H₂.
- The formation of soot is highly induced by the increase in H₂ and the strain rate.
- The chemical effects of H₂ and CO play an important role in the reduction of the maximum flame temperature and the formation of soot.

REFERENCES

[1] Kennedy, I.M. (2007). The health effects of combustion-generated aerosols. *Proceedings of the Combustion Institute*, 31(2): 2757-2770. <https://doi.org/10.1016/j.proci.2006.08.116>

[2] Appel, J., Bockhorn, H., Frenklach, M. (2000). Kinetic modeling of soot formation with detailed chemistry and physics: Laminar premixed flames of C₂ hydrocarbons. *Combustion and Flame*, 121(1-2): 122-136. [https://doi.org/10.1016/S0010-2180\(99\)00135-2](https://doi.org/10.1016/S0010-2180(99)00135-2)

[3] Xu, L., Yan, F., Zhou, M., Wang, Y., Chung, S.H. (2018). Experimental and soot modeling studies of ethylene counterflow diffusion flames: Non-monotonic influence of the oxidizer composition on soot formation. *Combustion and Flame*, 197: 304-318. <https://doi.org/10.1016/j.combustflame.2018.08.011>

[4] Wang, Y., Liu, X., Gu, M., An, X. (2018). Numerical simulation of the effects of hydrogen addition to fuel on the structure and soot formation of a laminar axisymmetric coflow C₂H₄/(O₂-CO₂) diffusion flame. *Combustion Science and Technology*, 191(10): 1743-1768. <https://doi.org/10.1080/00102202.2018.1532413>

[5] Guo, H., Liu, F., Smallwood, G.J., Gülder, Ö.L. (2006). Numerical study on the influence of hydrogen addition on soot formation in a laminar ethylene-air diffusion flame. *Combustion and Flame*, 145(1-2): 324-338. <https://doi.org/10.1016/j.combustflame.2005.10.016>

[6] Boussetla, S., Mameri, A., Hadeif, A. (2021). NO Emission from non-premixed MILD combustion of biogas-syngas mixtures in opposed jet configuration. *International Journal of Hydrogen Energy*, 46(75): 37641-37655.

<https://doi.org/10.1016/j.ijhydene.2021.01.074>

[7] Wang, Y., Gu, M., Chao, L., Wu, J., Lin, Y., Huang, X. (2021). Different chemical effect of hydrogen addition on soot formation in laminar coflow methane and ethylene diffusion flames. *International Journal of Hydrogen Energy*, 46(29): 16063-16074. <https://doi.org/10.1016/j.ijhydene.2021.02.014>

[8] Zhang, Y., Liu, F., Lou, C. (2018). Experimental and numerical investigations of soot formation in laminar coflow ethylene flames burning in O₂/N₂ and O₂/CO₂ atmospheres at Different O₂ mole fractions. *Energy & Fuels*, 32(5): 6252-6263. <https://doi.org/10.1021/acs.energyfuels.7b04069>

[9] Khanehazar, A., Cepeda, F., Dworkin, S.B. (2022). The influence of nitrogen and hydrogen addition/dilution on soot formation in coflow ethylene/air diffusion flames. *Fuel*, 309: 122244. <https://doi.org/10.1016/j.fuel.2021.122244>

[10] Liu, F., Ai, Y., Kong, W. (2014). Effect of hydrogen and helium addition to fuel on soot formation in an axisymmetric coflow laminar methane/air diffusion flame. *International Journal of Hydrogen Energy*, 39(8): 3936-3946. <https://doi.org/10.1016/j.ijhydene.2013.12.151>

[11] Ying, Y., Liu, D. (2015). Detailed influences of chemical effects of hydrogen as fuel additive on methane flame. *International Journal of Hydrogen Energy*, 40(9): 3777-3788. <https://doi.org/10.1016/j.ijhydene.2015.01.076>

[12] Wei, M., Liu, J., Guo, G., Li, S. (2016). The effects of hydrogen addition on soot particle size distribution functions in laminar premixed flame. *International Journal of Hydrogen Energy*, 41(14): 6162-6169. <https://doi.org/10.1016/j.ijhydene.2015.10.022>

[13] Lee, H.C., Mohamad, A.A., Jiang, L.Y. (2015). Comprehensive comparison of chemical kinetics mechanisms for syngas/biogas mixtures. *Energy & Fuels*, 29(9): 6126-6145. <https://doi.org/10.1021/acs.energyfuels.5b01136>

[14] Xu, L., Yan, F., Wang, Y., Chung, S.H. (2020). Chemical effects of hydrogen addition on soot formation in counterflow diffusion flames: Dependence on fuel type and oxidizer composition. *Combustion and Flame*, 213: 14-25. <https://doi.org/10.1016/j.combustflame.2019.11.011>

[15] Fisher, E.M., Williams, B.A., Fleming, J.W. (1997). Determination of the strain in counterflow diffusion flames from flow conditions. *Proceedings of the Eastern States Section of the Combustion Institute*, pp. 191-194.

[16] Lutz, A.E., Kee, R.J., Grcar, J.F., Rupley, F.M. (1996). OPPDIF: A Fortran program for computing opposed-flow diffusion flames. Report 96-8243. Sandia National Laboratories, Livermore, California, USA. <https://doi.org/10.2172/568983>

[17] Baukal Jr., C.E., Gershtein, V.Y., Li, X. (2000). *Computational Fluid Dynamics in Industrial Combustion*. CRC Press.

[18] Frenklach, M. (2002). Method of moments with interpolative closure. *Chemical Engineering Science*, 57(12): 2229-2239. [https://doi.org/10.1016/s0009-2509\(02\)00113-6](https://doi.org/10.1016/s0009-2509(02)00113-6)

[19] Kee, R.J., Miller, J.A., Evans, G.H., Dixon-Lewis, G. (1989). A computational model of the structure and extinction of strained, opposed flow, premixed methane-air flames. *Symposium (International) on Combustion*,

- 22(1): 1479-1494. [https://doi.org/10.1016/s0082-0784\(89\)80158-4](https://doi.org/10.1016/s0082-0784(89)80158-4)
- [20] Appel, J., Bockhorn, H., Frenklach, M. (2000). Kinetic modeling of soot formation with detailed chemistry and physics: laminar premixed flames of C₂ hydrocarbons. *Combustion and Flame*, 121(1-2): 122-136. [https://doi.org/10.1016/s0010-2180\(99\)00135-2](https://doi.org/10.1016/s0010-2180(99)00135-2)
- [21] Zhou, M., Yan, F., Ma, L., Jiang, P., Wang, Y., Chung, S.H. (2022). Chemical speciation and soot measurements in laminar counterflow diffusion flames of ethylene and ammonia mixtures. *Fuel*, 308: 122003. <https://doi.org/10.1016/j.fuel.2021.122003>
- [22] Wang, Y., Gu, M., Zhu, Y., Cao, L., Zhu, B., Wu, J., Lin, Y., Huang, X. (2021). A review of the effects of hydrogen, carbon dioxide, and water vapor addition on soot formation in hydrocarbon flames. *International Journal of Hydrogen Energy*, 46(61): 31400-31427. <https://doi.org/10.1016/j.ijhydene.2021.07.011>
- [23] Wang, Y., Gu, M., Gao, Y., Liu, X., Lin, Y. (2020). An experimental and numerical study of soot formation of laminar coflow H₂/C₂H₄ diffusion flames in O₂/CO₂ atmosphere. *Combustion and Flame*, 221: 50-63. <https://doi.org/10.1016/j.combustflame.2020.07.026>
- [24] He, D., Yan, W. (2018). Influences of different diluents on NO emission characteristics of syngas opposed-flow flame. *International Journal of Hydrogen Energy*, 43(5): 2570-2584. <https://doi.org/10.1016/j.ijhydene.2017.11.171>